

SENSITIVITY OF CELLULAR WIRELESS NETWORK PERFORMANCE TO SYSTEM & PROPAGATION PARAMETERS AT CARRIER FREQUENCIES GREATER THAN 2 GHz

K. A. Anang^{*}, P. B. Rapajic, L. Bello, and R. Wu

Wireless and Mobile Communication Research Centre, School of Engineering, University of Greenwich, Medway, Chatham Maritime, ME4 4TB, UK

Abstract—In this paper, mathematical analysis supported by computer simulation is used to investigate the impact of both system and propagation loss parameters on the performance of cellular wireless network operating at microwave carrier frequencies greater than 2 GHz, where multiple tier of co-channel interfering cells are considered to be active. The two-slope path loss model and the uplink information capacity of the cellular network is used for the performance analysis. Results show that for carrier frequencies greater than 2 GHz and smaller cell radius multiple tier of co-channel interfering cells become active as compared to carrier frequencies lesser than 2 GHz. The multiple tier of co-channel interfering cells, leads to a decrease in the information capacity of the cellular wireless network. The results also show that the system performance is sensitive to most of the propagation model parameters such as the basic and extra path loss exponent.

1. INTRODUCTION

In the past, wireless communication systems were required to accommodate a large number of voice and/or low-speed data service. Now emerging wireless communication systems requires high-speed data service. It is therefore important for emerging wireless systems to achieve a high degree of spectrum efficiency, because the radio spectrum available is limited and regulated by international agreements [1, 2].

Received 23 January 2012, Accepted 27 March 2012, Scheduled 4 April 2012

* Corresponding author: Kwashie Amartei Anang (k.anang@greenwich.ac.uk).

Cellular system is partly used to achieve high spectrum efficiency by exploiting the power falloff with distance of signal propagation to reuse the same frequency channel in a spatially separated location. Recently, multiple-input multiple-out (MIMO) systems which are based on the use of multiple antennas at each end of the communication link have received much interest because of their ability to increase the spectral efficiency [3, 4]. Now, in [5, 6], it was reported that future cellular wireless systems will need to operate at higher microwave carrier frequency to offer the required high speed data service for emerging wireless system.

However, higher microwave carrier frequency means cell radius need to be reduced to microcell or picocell, because of an increase in path loss. Reduction in cell size, however causes a problem of co-channel interference [7, 8]. At higher frequencies radio propagation are exposed to non-line-of-sight (non-LOS) condition, which is the typical mode of operation in today's urban cellular communications [9]. Therefore, at higher frequencies and smaller cell radii (ranging, few hundred meters to a kilometer) base station (BS) antennas are below rooftops of surrounding buildings and the radio link between the transmitter and the receiver is in the line of sight (LOS) [10]. Thus, making the characterization of propagation in microcells different from that in traditional cells (macrocells) [11]. Radiowave propagation are therefore best modeled using the two-slope path loss model, where there exist a LOS propagation between the transmitter and the receiver [12, 13].

Although the two-slope propagation model has been used for performance analysis for LOS microcellular systems, only a few works have investigated the effect of propagation parameters on the system performance [14, 15]. With the development of high-speed data wireless communication services, together with the limited radio spectrum available, there is a need for effective wireless network traffic engineering. However, to date to the best of our knowledge the few published papers addressing the effect of the propagation model parameters on the performance of LOS microcellular systems considered the first tier or first and second tier co-channel interfering cells to be active assuming all other co-channel interfering cells to be negligible [6, 16, 17].

These omissions in previous work motivated this work. Our main contribution in this work is as follows:

- We studied the impact of system parameters (such as cell size, antenna height, operating frequency, and reuse factor) on the information capacity of emerging cellular wireless systems which will be operating at carrier frequencies greater than 2 GHz, when

multiple tier of co-channel interfering cells are active.

- We investigated the impact of propagation loss parameters (such as breakpoint, effective road height, and path loss exponent) on the information capacity of emerging cellular wireless network operating at carrier frequencies greater than 2 GHz, when multiple tier interferers are active.

The rest of the paper is organized as follows. Section 2 describes the system models for propagation, multiple tier co-channel interference, user position; and outlines the basic assumptions used in the modeling. In Section 3, expressions for the area spectral efficiency (ASE), in frequency or time division multiple-access (F/TDMA), based microcellular systems is derived. Section 4 presents some analysis and simulation results. Finally, in Section 5, some conclusions are drawn from the simulation results.

2. PROPAGATION AND SYSTEM MODELS

A two-dimensional hexagonal non-sectorized microcellular network is assumed where the BSs' are uniformly distributed. All cells are assumed to have omnidirectional antennas. Figure 1 shows a cellular layout consisting of cell BS_0 which we refer to as the reference cell and n -tiers of co-channel interfering cells. Now a cell j is served by BS_j , which is located at the cells center, with $1 \leq j \leq 6$ for first tier co-channel interferes, $7 \leq j \leq 18$ for second tier co-channel interferes, and $[(n-1) \times 6] + 1 \leq j \leq [(n-1) \times 6] + 6n$ for the n th tier co-channel interferes. Let D (refer to Figure 1) stand for the distance between BS_0 and a first tier BS. A second tier BS is then at a distance of $2D$ from BS_0 . An n th tier BS will be located at distance nD . In this paper, we focus on the case when interference is determine by path loss.

2.1. Channel Model

Wireless channel are characterized by the following physical phenomena: (1) mean path loss, (2) shadowing (slow fading), and (3) small-scale fading (fast fading). Sánchez et al. in their work in [18], reported that a 'snapshot' measurement may seriously underestimate the maximum mean electromagnetic field level that may be reached at a particular location. However, they also stated that 'snapshot' measurement results may still be valid. Therefore, in this work for simplicity and because it is a first order prediction analysis, we average out slow fading and fast fading and consider only path loss, though fading may have a considerable impact on the results.

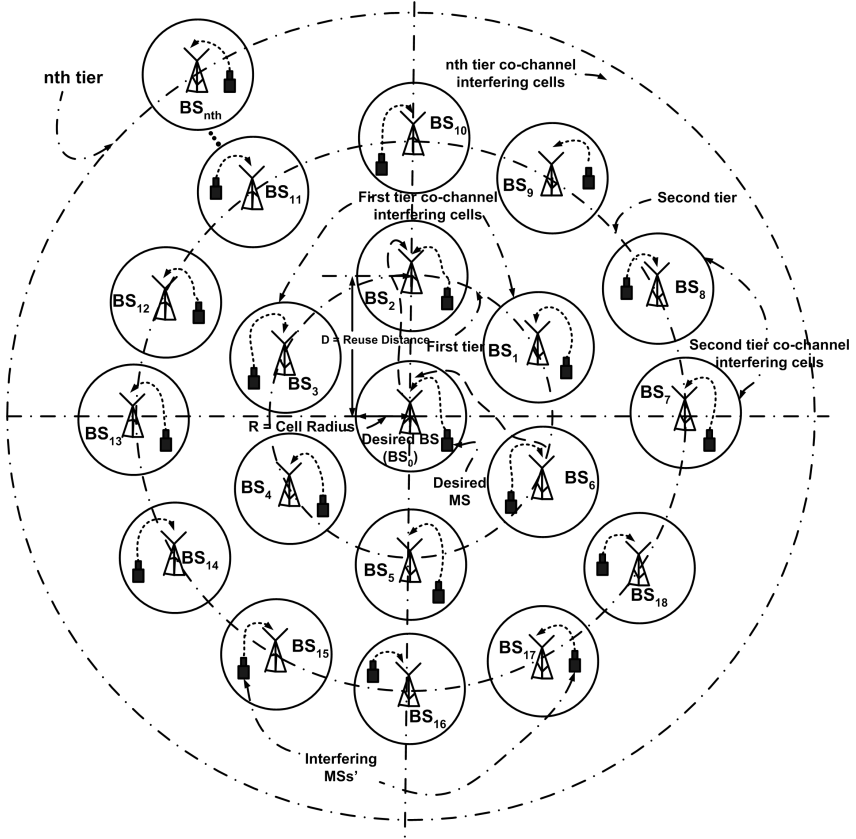


Figure 1. Cellular site layout with multiple tier co-channel interfering cells; cluster size $N_c = 7$.

In cellular network accurate modeling of path loss is required, because it is one of the major sources of systems performance degradation in cellular wireless system [19]. Now modeling radiowave propagation in LOS microcellular systems can be done by using the two-slope path loss model. Therefore, in this work, we adopt the following commonly used two-slope path loss model suggested by Harley [20]:

$$S_r = \frac{C}{r^\alpha(1+r/g)^\rho} S_t, \quad (1)$$

where S_r [W], is the received signal power, C is the constant factor of path loss, which depends on the antenna heights and carrier frequency, α is the basic path loss exponent (ranges from 2–4), for $r \leq g$, ρ is the

extra path loss exponent (ranges from 2–8), for $r > g$. The parameter r [m], is the separation distance between BS and mobile station (MS), S_t [W] is the transmitted signal power, and g [m] is the breakpoint of the path loss curve.

2.2. Breakpoint

The breakpoint distance g of the two-slope propagation model separates the different properties of propagation in the near and far regions relative to the BS. The breakpoint distance has been validated experimentally for both ultra high frequency (UHF) and super-high frequency (SHF) bands [21, 22], and it is proportional to the product of MS and BS antenna heights, h_m and h_b [m], and inversely proportional to the carrier wavelength λ_c of the transmitter source. g is given by [22], as

$$g = \frac{4h_b h_m}{\lambda_c} \tag{2}$$

In this work, we use the following typical values $h_m = 1.5$ m, $h_b = 15$, 35 and 55 m and $f_c = 0.9$, 2, 3.35 and 8.45 GHz [5, 23–25], which have been used in previous analysis. Figure 2 shows a plot of breakpoint

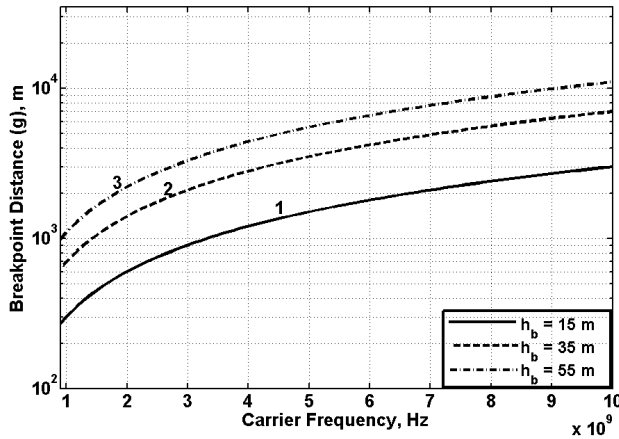


Figure 2. Breakpoint distance, g versus microwave carrier frequency f_c for different BS antenna heights h_b . ($h_b = 15$, 35 and 55 m and MS antenna height $h_m = 1.5$ m.).

1. BS antenna height, $h_b = 15$ m.
2. BS antenna height, $h_b = 35$ m.
3. BS antenna height, $h_b = 55$ m.

distance versus carrier frequency for different h_b . The curves show that for a given f_c , as h_b increases, g becomes longer.

2.3. User Distribution

Cell shape is approximated by a circle of radius R for analytical convenience. MSs' (desired and interfering) are assumed to be mutually independent and uniformly distributed in their respective cells. The probability distribution function (PDF) of a MS location polar coordinates (r, θ) relative to their BS's is given by [26] as

$$p_{r,\theta}(r, \theta) = \frac{(r - R_0)}{\pi(R - R_0)^2}; \quad R_0 \leq r \leq R, \quad 0 \leq \theta \leq 2\pi. \quad (3)$$

where R_0 [m] is the closet distance a MS can be from a BS antenna, and is approximately 20 m for microcellular networks.

2.4. Multiple Tier Co-channel Interference

Multiple tiers of co-channel interfering cells are considered for interference generation. The desired MS is in the central cell and interfering MSs' are in cells in the first, second and other tiers. Figure 1 shows a cellular site layout with n -tier co-channel interfering cells surrounding the desired BS (BS_0).

To simplify the analysis, because C in (1) is a constant, and is assumed to be the same for all interference, it is neglected without loss of generality. We assume here that terminal noise is negligible compared to interference [27]. Thereby, reducing the ratio of carrier to noise (CNR) to carrier-to-interference power ratio (CIR). All inter-channel interference are also considered to be negligible [27]. We assume all BSs' to transmit the same power, and each cell is assumed to be circular shape.

The desired user CIR , γ , is defined as the ratio of the average received signal power level, S_r [W] from a MS at a distance r [m] from the desired BS to the sum S_I [W] of interfering power at distances $r_{i1}, r_{i2}, \dots, r_{in}$ from the interfering BSs'. The desired user CIR , γ , can therefore be written as

$$\gamma = \frac{S_r}{S_I} = \frac{S_r(r)}{\sum_{i1=1}^{N_{I1}} S_{i1}(r_{i1}) + \sum_{i2=1}^{N_{I2}} S_{i2}(r_{i2}) + \dots + \sum_{in=1}^{N_{IN}} S_{in}(r_{in})}. \quad (4)$$

where S_{i1} , S_{i2} and S_{in} [W] are the average received power from the n th interfering BSs'. N_{I1} , N_{I2} , \dots , N_{IN} are the number of co-channel interfering cells in the respective tiers.

3. AREA SPECTRAL EFFICIENCY

The area spectral efficiency (ASE) of a cell is defined as the achievable sum rate per unit bandwidth per unit area. The ASE is given by [26] as:

$$A_e = \frac{\sum_{k=1}^{N_s} C_k}{\pi B(D/2)^2} \quad (5)$$

where B is the total bandwidth allocated to each cell, D is the reuse distance, N_s is the total number of active serviced channels per cell. The achievable sum rate C_k is the Shannon capacity of the k th user and it depends on γ which is the received *CIR* of that user, and B_k the bandwidth allocated to the user. The Shannon capacity formula assumes interference has Gaussian characteristics. Because both the interference and signal power of the k th user vary with mobiles locations and propagation conditions, γ varies with time, therefore the average channel capacity of the k th user is given by [26] as

$$\langle C_k \rangle = B_k \int_0^{+\infty} \log_2(1 + \gamma) p_\gamma(\gamma) d\gamma, \quad (6)$$

where $p_\gamma(\gamma)$, is the PDF of the average mean *CIR* (γ) of the k th user.

We assumed transmission rate to be continuously adapted relative to the *CIR* in such a manner that the *BER* goes to zero asymptotically. In (6), assuming that all users are assigned the same bandwidth, $\langle C_k \rangle = \langle C \rangle$ becomes the same for all users, therefore $\langle A_e \rangle$ can be written as

$$\langle A_e \rangle = \frac{4N_s \langle C \rangle}{\pi B D^2} = \frac{4N_s \langle C \rangle}{\pi B R_u^2 R^2}, \quad (7)$$

where R_u is defined as the *normalized reuse distance* and is given by the ratio of reuse distance and cell radius (D/R). Now considering a FDMA systems, where all users are given the same bandwidth $B_k = B_0 = B/N_s$. Substituting B/N_s in (6) followed by substitution into (7) yields

$$\langle A_e \rangle = \frac{4}{\pi R_u^2 R^2} \int_0^{+\infty} \log_2(1 + \gamma) p_\gamma(\gamma) d\gamma. \quad (8)$$

4. PROPAGATION/SYSTEM PARAMETER IMPACT ANALYSIS

Our analysis applies to bandwidth limited systems such as FDMA and TDMA. It is based on a fully loaded non-sectorized cellular wireless

system. However our analysis can easily be applied to sectorized cellular systems which have been studied extensively in [28]. In our analysis the effect of shadowing and multipath fading have been ignored for simplicity. Although there is an excessive demand to broadcast (downlink) high speed data in most emerging communication services, without loss generality we consider only the uplink between a MS and an intended BS.

4.1. Analysis

The analysis so far, shows that γ is a function of received signal power from the desired and interfering users. Since the desired MS's and interfering MSs' are randomly located, γ is also a random variable (RV). In smaller cell size wireless environment, frequencies are reused over a urban area with different cluster size N_c . For $N_c = 7$, the number of co-channel interfering cell in the first tier is 6. The number of subsequent tier co-channel interfering cells is given by $6 \times n$ [29], where n is the n th tier. Equation (4), can now be written as follows:

$$\gamma = \frac{S_r(r)}{\sum_{i1=1}^6 S_{i1}(r_{i1}) + \sum_{i2=1}^{6.2} S_{i2}(r_{i2}) + \dots + \sum_{in=1}^{6.n} S_{in}(r_{in})}. \quad (9)$$

Table 1. Simulation parameters.

Parameter	Value
Cell radius	100 to 1000 m
Path loss exponent (α)	2, 2.5, and 3
Additional path loss exponent (ρ)	2, 4, 5 and 8
BS antenna height	15, 35 and 55 m [23]
MS antenna height	1.5 m [25]
Mobile Distribution	Uniform/Random
Number of co-channel tiers	10
Co-channel interferences	Random and multiple tiers
Frequency reuse factor (R_u)	4 [26]
Carrier frequencies (f_c)	0.9, 2, 3.35 and 8.45 GHz [5, 24]

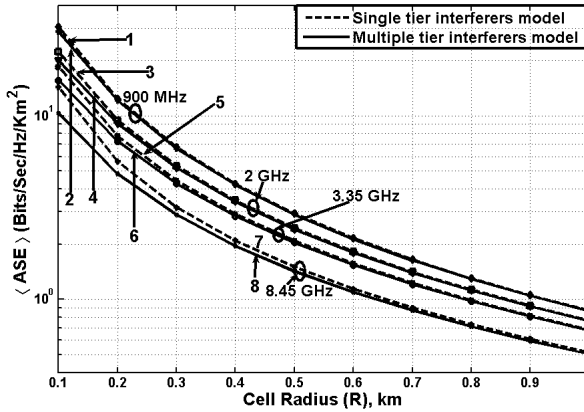


Figure 3. Uplink ASE as a function of cell radius R , for different carrier frequency f_c and path loss exponent $\alpha = 2$. (Fully loaded system; extra path loss exponent $\rho = 4$; normalized reuse distance $R_u = 4$, BS antenna heights $h_b = 15$ and MS antenna height $h_m = 1.5$ m; number of co-channel interfering cells; single tier = 6 and multiple tier = 330.)

1. Single tier interferers model, ($f_c = 900$ MHz).
2. Multiple tier interferers model, ($f_c = 900$ MHz).
3. Single tier interferers model, ($f_c = 2$ GHz).
4. Multiple tier interferers model, ($f_c = 2$ GHz).
5. Single tier interferers model, ($f_c = 3.35$ GHz).
6. Multiple tier interferers model, ($f_c = 3.35$ GHz).
7. Single tier interferers model, ($f_c = 8.45$ GHz).
8. Multiple tier interferers model, ($f_c = 8.45$ GHz).

Using the summation properties and assuming the transmitted power of all MSs' to be the same and substituting (1) in (9) yields

$$\gamma = \frac{r^{-\alpha}(1 + r/g)^{-\rho}}{\sum_{n=1}^{\infty} \sum_{i=1}^{6.n} (nR_u R_{ni})^{-\alpha} (1 + nR_u R_{ni}/g)^{-\rho}}. \quad (10)$$

Keeping in mind that the average CIR of the desired MS, γ , is a function of both the total number of interferers N_T , and the desired MS's position, r , the desired MS's capacity is given as

$$\bar{C}(N_T, r) = B \log_2(1 + \bar{\gamma}(N_T, r)). \quad (11)$$

Without power control, all the N_T co-channel interferers are at the center of their respective cells (average case interference). Integrating (11) over the desired MS's position PDF (3) yields the average ASE for the average interference configuration as:

$$\bar{A}_e(N_T) = \frac{4}{\pi R_u^2 R^2} \int_{R_0}^R \log_2(1 + \bar{\gamma}(N_T, r) p_r(r)) dr. \quad (12)$$

It is mathematically intractable to solve the integral in (12), as the average ASE depends on γ which is a function of random locations of MSs'. A Monte Carlo simulation is therefore used to solve it.

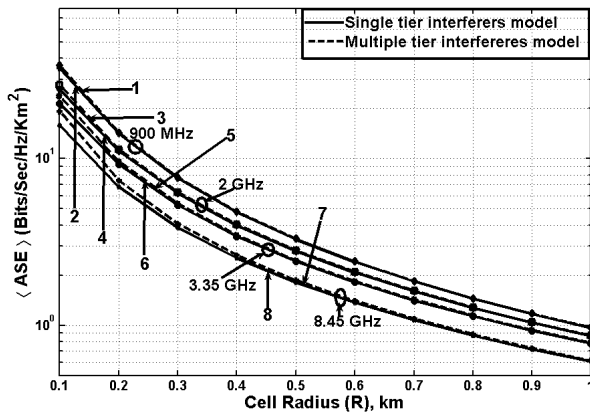


Figure 4. Uplink ASE as a function of cell radius R , for different carrier frequency f_c and path loss exponent $\alpha = 2.5$. (Fully loaded system; extra path loss exponent $\rho = 4$; normalized reuse distance $R_u = 4$, BS antenna heights $h_b = 15$ and MS antenna height $h_m = 1.5$ m; number of co-channel interfering cells; single tier = 6 and multiple tier = 330.)

1. Single tier interferers model, ($f_c = 900$ MHz).
2. Multiple tier interferers model, ($f_c = 900$ MHz).
3. Single tier interferers model, ($f_c = 2$ GHz).
4. Multiple tier interferers model, ($f_c = 2$ GHz).
5. Single tier interferers model, ($f_c = 3.35$ GHz).
6. Multiple tier interferers model, ($f_c = 3.35$ GHz).
7. Single tier interferers model, ($f_c = 8.45$ GHz).
8. Multiple tier interferers model, ($f_c = 8.45$ GHz).

4.2. Simulations

As \bar{A}_e appears to be mathematically intractable to solve explicitly analytically, a Monte Carlo simulation is therefore used to estimate it. The basic parameter used for the simulations are summarized in Table 1. We considered only ten tiers of co-channel interfering cells for simulation, because by successive numerical runs with an increasing number of tiers, we found that the addition of further tiers beyond ten had no effect on the accuracy of our results. The simulation methodology is as follows:

- (i) The polar coordinates (x_{ni}, θ_{ni}) of the N_{ni} co-channel interferer is randomly picked according to (3).

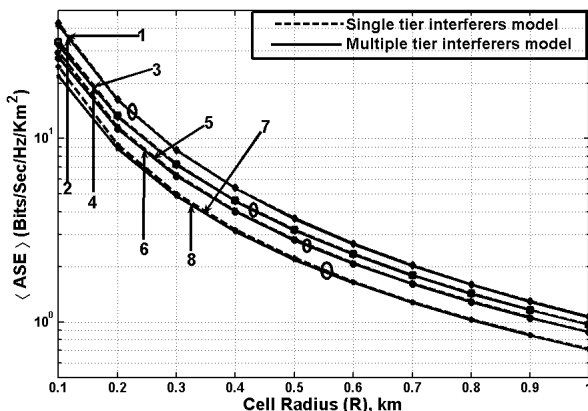


Figure 5. Uplink ASE as a function of cell radius R , for different carrier frequency f_c and path loss exponent $\alpha = 3$. (Fully loaded system; extra path loss exponent $\rho = 4$; normalized reuse distance $R_u = 4$, BS antenna heights $h_b = 15$ and MS antenna height $h_m = 1.5$ m; number of co-channel interfering cells; single tier = 6 and multiple tier = 330.)

1. Single tier interferers model, ($f_c = 900$ MHz).
2. Multiple tier interferers model, ($f_c = 900$ MHz).
3. Single tier interferers model, ($f_c = 2$ GHz).
4. Multiple tier interferers model, ($f_c = 2$ GHz).
5. Single tier interferers model, ($f_c = 3.35$ GHz).
6. Multiple tier interferers model, ($f_c = 3.35$ GHz).
7. Single tier interferers model, ($f_c = 8.45$ GHz).
8. Multiple tier interferers model, ($f_c = 8.45$ GHz).

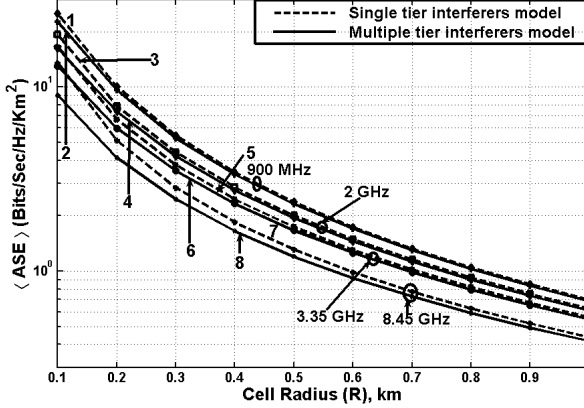


Figure 6. Uplink ASE as a function of cell radius R , for different carrier frequency f_c and extra path loss exponent $\rho = 3$. (Fully loaded system; path loss exponent $\alpha = 2$; normalized reuse distance $R_u = 4$, BS antenna heights $h_b = 15$ and MS antenna height $h_m = 1.5$ m; number of co-channel interfering cells; single tier = 6 and multiple tier = 330.)

1. Single tier interferers model, ($f_c = 900$ MHz).
2. Multiple tier interferers model, ($f_c = 900$ MHz).
3. Single tier interferers model, ($f_c = 2$ GHz).
4. Multiple tier interferers model, ($f_c = 2$ GHz).
5. Single tier interferers model, ($f_c = 3.35$ GHz).
6. Multiple tier interferers model, ($f_c = 3.35$ GHz).
7. Single tier interferers model, ($f_c = 8.45$ GHz).
8. Multiple tier interferers model, ($f_c = 8.45$ GHz).

(ii) The received power from each i th interfering MS is calculated as:

$$r_{ni} = \sqrt{nD^2 + x_{ni}^2 - 2nDx_{ni} \cos(\theta_{ni})}. \quad (13)$$

(iii) The CIR of the desired MS $\gamma(r)$ is calculated as:

$$\gamma(r) = \frac{r^{-\alpha}(1 + r/g)^{-\rho}}{\sum_{i=1}^{10} \sum_{n=1}^{6.n} (jr_{ni})^{-\alpha}(1 + nr_{ni}/g)^{-\rho}}. \quad (14)$$

(iv) The average ASE, \bar{A}_e is calculated as:

$$\bar{A}_e(r) = \frac{4}{\pi R_u^2 R^2} \log_2(1 + \gamma(r)). \quad (15)$$

We repeat the above process 100, 000 times and average all the values to get an estimate of \bar{A}_e .

4.3. Simulations Results

In this section, we present simulation results to show the effect of propagation loss parameters and system parameters on the performance of microcellular systems operating at carrier frequencies greater than 2 GHz, where multiple tier co-channel interference are active.

In Figure 3, we compare the ASE for the single and multiple tier co-channel interference models for different f_c , when $\alpha = 2$. The

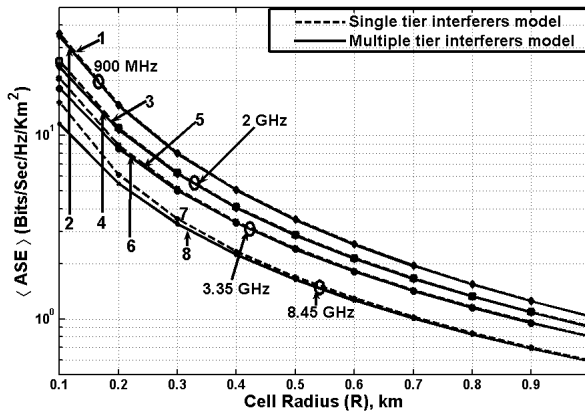


Figure 7. Uplink ASE as a function of cell radius R , for different carrier frequency f_c and extra path loss exponent $\rho = 5$. (Fully loaded system; path loss exponent $\alpha = 2$; normalized reuse distance $R_u = 4$, BS antenna heights $h_b = 15$ and MS antenna height $h_m = 1.5$ m; number of co-channel interfering cells; single tier = 6 and multiple tier = 330.)

1. Single tier interferers model, ($f_c = 900$ MHz).
2. Multiple tier interferers model, ($f_c = 900$ MHz).
3. Single tier interferers model, ($f_c = 2$ GHz).
4. Multiple tier interferers model, ($f_c = 2$ GHz).
5. Single tier interferers model, ($f_c = 3.35$ GHz).
6. Multiple tier interferers model, ($f_c = 3.35$ GHz).
7. Single tier interferers model, ($f_c = 8.45$ GHz).
8. Multiple tier interferers model, ($f_c = 8.45$ GHz).

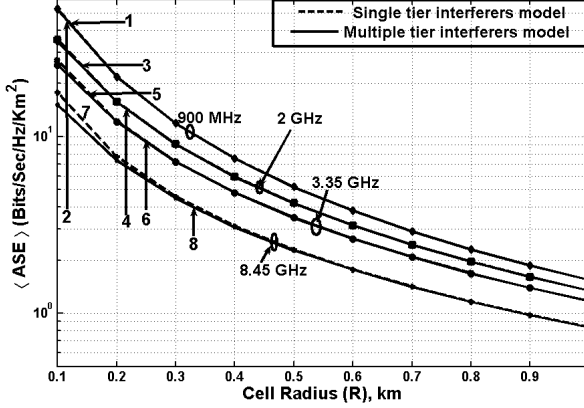


Figure 8. Uplink ASE as a function of cell radius R , for different carrier frequency f_c and extra path loss exponent $\rho = 8$. (Fully loaded system; path loss exponent $\alpha = 2$; normalized reuse distance $R_u = 4$, BS antenna heights $h_b = 15$ and MS antenna height $h_m = 1.5$ m; number of co-channel interfering cells; single tier = 6 and multiple tier = 330.)

1. Single tier interferers model, ($f_c = 900$ MHz).
2. Multiple tier interferers model, ($f_c = 900$ MHz).
3. Single tier interferers model, ($f_c = 2$ GHz).
4. Multiple tier interferers model, ($f_c = 2$ GHz).
5. Single tier interferers model, ($f_c = 3.35$ GHz).
6. Multiple tier interferers model, ($f_c = 3.35$ GHz).
7. Single tier interferers model, ($f_c = 8.45$ GHz).
8. Multiple tier interferers model, ($f_c = 8.45$ GHz).

curves show that when $f_c = 900$ MHz and $R = 0.1$ km, there was a 5.67% decrease in ASE between the single and multiple interferers model, at 0.3 km the decrease was 1.47% and still lesser for greater values of R . For $f_c = 2$ GHz at 0.1 km the decrease in ASE was 10.45% and for 0.3 km it was 2.46% and lesser still for greater values R . At 3.35 GHz, the decrease was 15.60% and 3.78% at 0.1 and 0.3 km. Now for 8.45 GHz the decrease in ASE was 27.86% at 0.1 km, 9.05% at 0.3 km, 4.13% at 0.6 km and 2.74% at 0.8 km and lesser still for greater values of R .

Figure 4 compares the ASE for the two models, when $\alpha = 2.5$. At $f_c = 900$ MHz and 0.1 km the decrease was 3.78% and lesser for greater values of R . For 2 GHz at 0.1 km the decrease was 6.88%, at 0.3 km it

was 1.43% and lesser for greater values of R . For $f_c = 3.35$ GHz the decrease was 10.00% and 2.23% at 0.1 and 0.3 km. At 8.45 GHz and 0.1 km the decrease in ASE was 17.69% at 0.3 km it was 5.26% and at 0.6 km was 2.86% and lesser for greater values of R .

Figure 5 compares the ASE for the two models, when $\alpha = 3$. At $f_c = 900$ MHz, 2 GHz and 3.35 GHz for $R = 0.1$ km the decrease in ASE between the two models was 2.60%, 4.51% and 6.49% and lesser than 1.5% for $R = 0.3$ km. However, at 8.45 GHz at 0.1 km there was 11.18% decrease in ASE and for 0.3 km it was 3.2% and still lesser for greater values of R . From the graphs we can conclude that at carrier frequencies greater than 2 GHz; at lower path loss exponent and smaller cell radius, multiple tiers of co-channel interfering cells become active, causing a decrease in ASE.

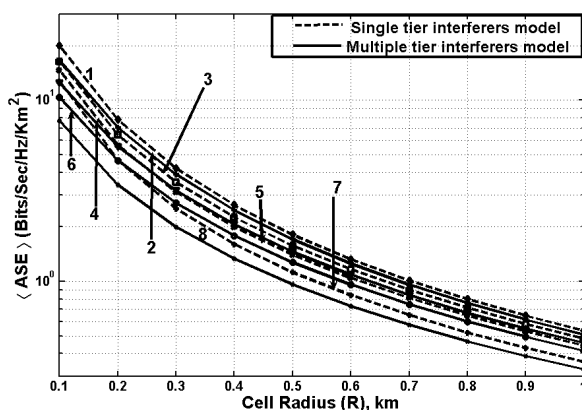


Figure 9. Uplink ASE as a function of cell radius R , for different carrier frequency f_c and BS antenna height $h_b = 15$ m. (Fully loaded system; path loss exponent $\alpha = 2$ and extra path loss exponent $\rho = 2$; normalized reuse distance $R_u = 4$; MS antenna height $h_m = 1.5$ m; number of co-channel interfering cells; single tier = 6 and multiple tier = 330.)

1. Single tier interferers model, ($f_c = 900$ MHz).
2. Multiple tier interferers model, ($f_c = 900$ MHz).
3. Single tier interferers model, ($f_c = 2$ GHz).
4. Multiple tier interferers model, ($f_c = 2$ GHz).
5. Single tier interferers model, ($f_c = 3.35$ GHz).
6. Multiple tier interferers model, ($f_c = 3.35$ GHz).
7. Single tier interferers model, ($f_c = 8.45$ GHz).
8. Multiple tier interferers model, ($f_c = 8.45$ GHz).

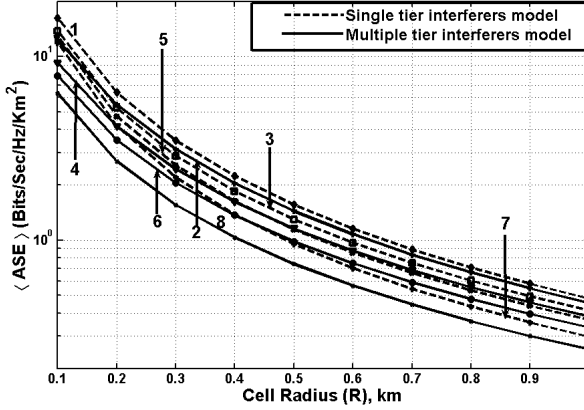


Figure 10. Uplink ASE as a function of cell radius R for different carrier frequency f_c and BS antenna height $h_b = 35$ m. (Fully loaded system; path loss exponent $\alpha = 2$ and extra path loss exponent $\rho = 2$; normalized reuse distance $R_u = 4$; and MS antenna height $h_m = 1.5$ m; number of co-channel interfering cells; single tier = 6 and multiple tier = 330.)

1. Single tier interferers model, ($f_c = 900$ MHz).
2. Multiple tier interferers model, ($f_c = 900$ MHz).
3. Single tier interferers model, ($f_c = 2$ GHz).
4. Multiple tier interferers model, ($f_c = 2$ GHz).
5. Single tier interferers model, ($f_c = 3.35$ GHz).
6. Multiple tier interferers model, ($f_c = 3.35$ GHz).
7. Single tier interferers model, ($f_c = 8.45$ GHz).
8. Multiple tier interferers model, ($f_c = 8.45$ GHz).

Figures 6–8 depicts the effect of the extra path loss exponent, ρ on the ASE and confirms that ASE increases as ρ becomes bigger, which is verified in [26], for a different model and also holds for our multiple tier interferers model, because ρ effects the far field interferer.

The curves in Figure 6 shows that for $\rho = 3$ and $f_c = 900$ MHz, the difference in ASE between the two interferers model was 9.60% and 3.12% for 0.1 and 0.3 km, whereas for 2 GHz at $R = 0.1$ km there was 15.58% decrease in ASE between the two models and at $R = 0.3$ km the decrease was 4.75%. At $f_c = 3.35$ GHz, the decrease in ASE between the two models was 21.21% at 0.1 km and 6.65% at 0.3 km. For $f_c = 8.45$ GHz, the decrease in ASE between the two models was 33.09% at 0.1 km and 13.38% at 0.3 km.

Figure 7 shows that for $\rho = 5$ and $f_c = 900$ MHz and 2 GHz, there was no much difference in ASE as compared to when $f_c = 3.35$ and 8.4 GHz. For 3.35 GHz the decrease was 11.66% for 0.1 km and for 8.45 GHz the decrease in ASE between the two models at 0.1 km was 23.63% and 6.00% at 0.3 km. Figure 8 shows that for $\rho = 8$ and $f_c = 900$ MHz, 2 GHz and 3.35 GHz, there was no much difference in ASE between the single and multiple tier interferers model, however, at 8.45 GHz there was a decrease of 14.86% at $R = 0.1$ km and 2.19% at $R = 0.3$ km. An important conclusion derived from Figures 6–8, is that at higher carrier frequencies and smaller extra path loss exponent other tiers of co-channel interfering cells apart from those in

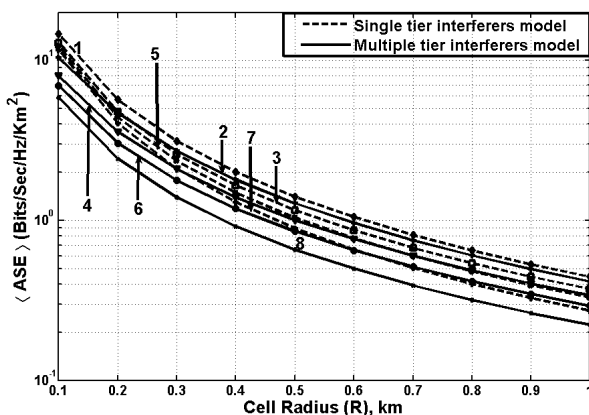


Figure 11. Uplink ASE as a function of cell radius R for different carrier frequency f_c and BS antenna height $h_b = 55$ m. (Fully loaded system; path loss exponent $\alpha = 2$ and extra path loss exponent $\rho = 2$; normalized reuse distance $R_u = 4$; and MS antenna height $h_m = 1.5$ m; number of co-channel interfering cells; single tier = 6 and multiple tier = 330.)

1. Single tier interferers model, ($f_c = 900$ MHz).
2. Multiple tier interferers model, ($f_c = 900$ MHz).
3. Single tier interferers model, ($f_c = 2$ GHz).
4. Multiple tier interferers model, ($f_c = 2$ GHz).
5. Single tier interferers model, ($f_c = 3.35$ GHz).
6. Multiple tier interferers model, ($f_c = 3.35$ GHz).
7. Single tier interferers model, ($f_c = 8.45$ GHz).
8. Multiple tier interferers model, ($f_c = 8.45$ GHz).

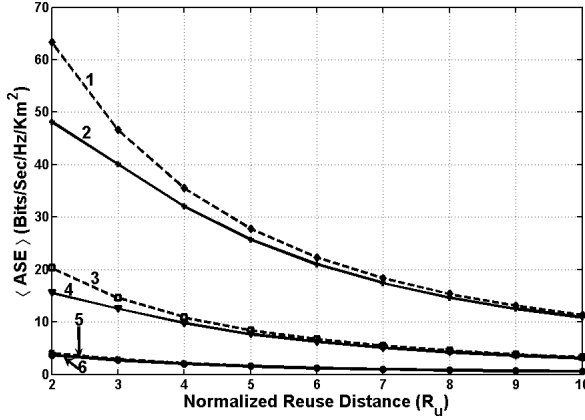


Figure 12. Comparison of the average ASE for single and multiple tier interferers model for different normalized reuse distances R_u and cell radius R . (Fully loaded system; carrier frequency $f_c = 900$ MHz; path loss exponent $\alpha = 2$ and extra path loss exponent $\rho = 2$; BS antenna height $h_b = 15$ m and MS antenna height $h_m = 1.5$ m; number of co-channel interfering cells; single tier = 6 and multiple tier = 330.)

1. Single tier interferers model, $R = 100$ m.
2. Multiple tier interferers model, $R = 100$ m.
3. Single tier interferers model, $R = 200$ m.
4. Multiple tier interferers model, $R = 200$ m.
5. Single tier interferers model, $R = 500$ m.
6. Multiple tier interferers model, $R = 500$ m.

the first tier becomes active. Because as carrier frequency increases the breakpoint distance of the two-slope path loss model increases (refer to Figure 2) allowing other co-channel interfering cells to be in the same region (basic path loss exponent, (α) region) as those of the first tier.

In Figures 9–11, the ASE is plotted as a function of the cell radius for different BS antenna heights, $\alpha = 2$, $\rho = 2$ and $f_c = 0.9, 2, 3.35$ and 8.45 GHz. In Figure 9, we compare the ASE for the single and multiple tier co-channel interference models for $f_c = 900$ Hz and $h_b = 15$ m. The curves show a decrease of 17.17% in ASE at $R = 0.1$ km, 5.52% for 0.5 km, and greater values of R lead to negligible decrease in ASE between the two interferer models. At 2 GHz and $R = 0.1$ km the curves show a decrease in ASE of 23.89% and 7.01% at 0.5 km and lesser for greater values of R . At $f_c = 3.35$ GHz, the decrease in ASE between the two interferers model was 29.37% and 9.29% for $R = 0.1$

and 0.5 km. For 8.45 GHz, the decrease was 39.47% at 0.1 km and 10.70% at 0.5 km.

Figure 10 compares the ASE for the two models, when $h_b = 35$ m. For $f_c = 900$ MHz, the curves show that at $R = 0.1$ km the decrease in ASE was 24.41% and for 0.5 km it was 7.69% and lesser for greater values of R . At 2 GHz and $R = 0.1$ km the curves show a decrease in ASE of 33.02% and 10.07% at 0.5 km and lesser for greater values of R . At 3.35 GHz and $R = 0.1$ and 0.5 km the decrease was 38.74% and 14.04%. For 8.45 GHz, at $R = 0.1$ and 0.5 km the decrease in ASE was 46.89% and 22.11%.

Figure 11 compares the ASE for the two models, when $h_b = 55$ m. For $f_c = 900$ Hz. The curves show that at $R = 0.1$ and 0.5 km the decrease in ASE was 29.22 and 9.22%. At $f_c = 2$ GHz, the curves show that at $R = 0.1$ and 0.5 km the decrease in ASE was 38.05% and

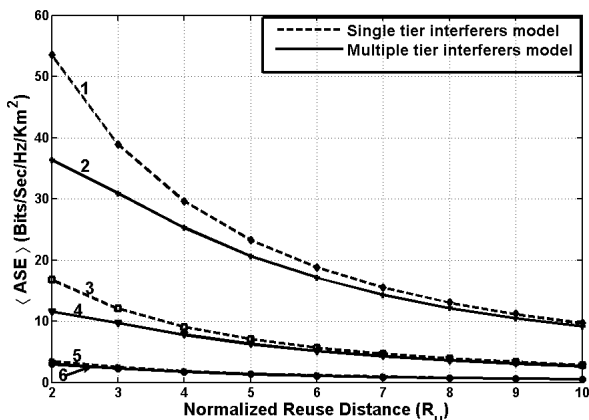


Figure 13. Comparison of the average ASE for single and multiple tier interferers model for different normalized reuse distances R_u and cell radius R . (Fully loaded system; carrier frequency $f_c = 2$ GHz; path loss exponent $\alpha = 2$ and extra path loss exponent $\rho = 2$; BS antenna height $h_b = 15$ m and MS antenna height $h_m = 1.5$ m; number of co-channel interfering cells; single tier = 6 and multiple tier = 330.)

1. Single tier interferers model, $R = 100$ m.
2. Multiple tier interferers model, $R = 100$ m.
3. Single tier interferers model, $R = 200$ m.
4. Multiple tier interferers model, $R = 200$ m.
5. Single tier interferers model, $R = 500$ m.
6. Multiple tier interferers model, $R = 500$ m.

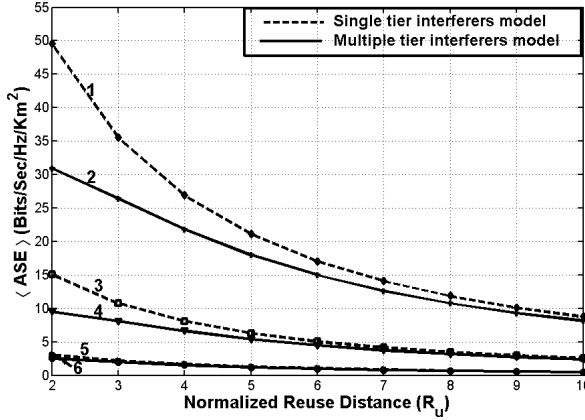


Figure 14. Comparison of the average ASE for single and multiple tier interferers model for different normalized reuse distances R_u and cell radius R . (Fully loaded system; carrier frequency $f_c = 3.35$ GHz; path loss exponent $\alpha = 2$ and extra path loss exponent $\rho = 2$; BS antenna height $h_b = 15$ m and MS antenna height $h_m = 1.5$ m; number of co-channel interfering cells; single tier = 6 and multiple tier = 330.)

1. Single tier interferers model, $R = 100$ m.
2. Multiple tier interferers model, $R = 100$ m.
3. Single tier interferers model, $R = 200$ m.
4. Multiple tier interferers model, $R = 200$ m.
5. Single tier interferers model, $R = 500$ m.
6. Multiple tier interferers model, $R = 500$ m.

13.79%, likewise for $f_c = 3.35$ GHz, at $R = 0.1$ and 0.5 km the decrease in ASE was 43.11% and 18.27%. For 8.45 GHz, the curves show that at $R = 0.1$ km the decrease in ASE was 49.40% and for 0.5 km it was 25.84%.

By examination of Figures 9–11, it can be concluded that at carrier frequencies greater than 2 GHz as the BS antenna height increases co-channel interference from other tiers becomes active, thus causing a decreasing in ASE.

Figures 12–15 illustrates the effect of the reuse pattern and the cell radius on the performance of a LOS microcellular wireless network. The figures confirms that the average ASE is an increasing function of reuse factor. The curves show that the decrease in ASE between the two interferers model at carrier frequency of 900 MHz was lesser as compared to those at 2, 3.35 and 8.45 GHz, this illustrate that the other

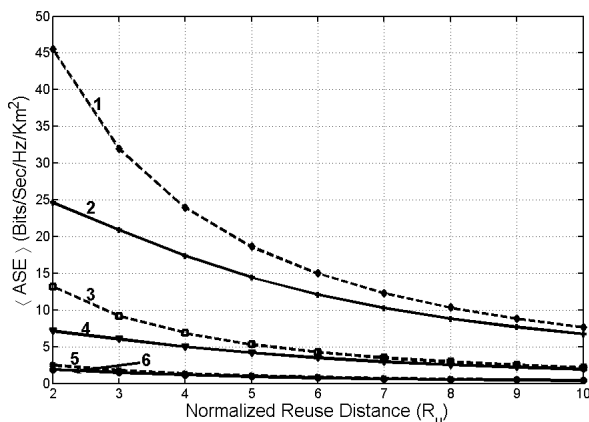


Figure 15. Comparison of the average ASE for single and multiple tier interferers model for different normalized reuse distances R_u and cell radius R . (Fully loaded system; carrier frequency $f_c = 8.45$ GHz; path loss exponent $\alpha = 2$ and extra path loss exponent $\rho = 2$; BS antenna height $h_b = 15$ m and MS antenna height $h_m = 1.5$ m; number of co-channel interfering cells; single tier = 6 and multiple tier = 330.)

1. Single tier interferers model, $R = 100$ m.
2. Multiple tier interferers model, $R = 100$ m.
3. Single tier interferers model, $R = 200$ m.
4. Multiple tier interferers model, $R = 200$ m.
5. Single tier interferers model, $R = 500$ m.
6. Multiple tier interferers model, $R = 500$ m.

tier co-channel interfering cells caused the ASE to decrease more at higher microwave carrier frequency. Also the decrease in ASE becomes larger as the cell size reduces. This illustrates the fact that the ASE depends on the cell size and also on the carrier frequency.

5. CONCLUSION

In this paper, we have analyzed and investigated the impact of both system and propagation parameters on the performance of FDMA/TDMA based LOS microcellular wireless networks operating at carrier frequencies greater than 2 GHz, when multiple tiers of co-channel interferers are active. Our performance analysis was based on the two-slope propagation loss model and the characterization of ASE as a function of cell radius.

The investigation showed that as carrier frequency increases; BS

antenna height increases; cell size reduces; basic path loss exponent decreases and extra path loss exponent decreases; multiple tiers of cochannel interfering cells become active, which causes a reduction in the uplink information capacity of a cellular wireless network.

The results from this paper show that the performance of cellular wireless network is sensitive to most of the propagation parameters, hence it is imperative to have a proper characterization of the propagation conditions to accurately plan and design a cellular network. Also the results show that for emerging cellular wireless network, which will be operating at carrier frequencies greater than 2 GHz, there is a need to include other tier co-channel interfering cells in the system model for accurate planning and design of the cellular network. In future work, we will incorporate more realistic assumptions such as sectorization, shadowing, correlation and multipath fading, because power control helps to ensure efficient spectral reuse and interference management it will also be considered in our future work.

REFERENCES

1. Lee, W. C. Y., "Spectrum efficiency in cellular [radio]," *IEEE Trans. Veh. Technol.*, Vol. 38, 69–75, May 1989.
2. Pahlavan, K. and A. H. Levesque, "Wireless data communication," *Proc. IEEE*, Vol. 82, 1398–1430, Sept. 1994.
3. Driessen, P. F. and G. J. Foschini, "On the capacity formula for multiple input-multiple output wireless channels: A geometric interpretation," *IEEE Trans. Commun.*, Vol. 47, No. 2, 173–176, Feb. 1999.
4. Molisch, A. F., *Wireless Communication*, 31, John Wiley & Sons, New York, 2005.
5. Masui, H., T. Kobayashi, and M. Akaike, "Microwave path-loss modeling in urban line-of-sight environments," *IEEE J. Select. Areas Commun.*, Vol. 20, No. 6, 1151–1155, Aug. 2002.
6. Hernández-Valdez, G., F. A. Cruz-Pérez, and D. Lara-Rodríguez, "Sensitivity of the system performance to the propagation parameters in LOS microcellular environments," *IEEE Trans. Veh. Technol.*, Vol. 57, No. 6, 3488–3508, Nov. 2008.
7. Jakes, W. C., *Microwave Mobile Communications*, 100–142, John Wiley & Sons, New York, 1994.
8. Takada, J., J. Fu, H. Zhu, and T. Kobayashi, "Spatiotemporal channel characterization in a suburban non line-of-sight microcellular environment," *IEEE J. Select. Areas Commun.*, Vol. 20, No. 3, 532–538, Apr. 2002.

9. Pabst, R., B. H. Walke, D. C. Schultz, P. Herhold, S. Mukherjee, H. Viswanathan, M. Lott, W. Zirwas, M. Dohler, H. Aghvami, D. D. Falconer, and G. P. Fettweis, "Relay-based deployment concepts for wireless and mobile broadband radio," *IEEE Commun. Mag.*, Vol. 42, No. 9, 80–89, Sept. 2004.
10. Kitao, K. and S. Ichitsubo, "Path loss prediction formula for microcell in 400 MHz to 8 GHz band," *Electron. Lett.*, Vol. 40, No. 11, 685–686, May 2004.
11. Goldsmith, A. J. and J. Greenstein, "A measurement-based model for predicting coverage areas of urban microcells," *IEEE J. Select. Areas Commun.*, Vol. 11, No. 7, 1013–1023, Sept. 1993.
12. Xia, H. H., H. L. Bertoni, L. R. Maciel, A. Lindsay-Stewart, and R. Rowe, "Radio propagation characteristics for line-of-sight microcellular and personal communications," *IEEE Trans. Antennas Propagat.*, Vol. 41, No. 10, 1439–1447, Oct. 1993.
13. Oda, Y., K. Tsunekawa, and M. Hata, "Advanced los pathloss model in microcellular mobile communications," *IEEE Trans. Veh. Technol.*, Vol. 49, No. 6, 2121–2125, Nov. 2000.
14. Ho, C., J. Copeland, C. Lea, and G. Stuber, "Impact of the cell size on the cell's Erlang capacity and call admission control in the ds/cdma cellular networks," *Proc. IEEE Veh. Technol. Conf.*, Vol. 1, 385–389, May 2000.
15. Cruz-Perez, F. A., D. Lara-Rodriguez, and M. Lara, "Full- and half-square cell plans in urban CDMA microcellular networks," *IEEE Trans. Veh. Technol.*, Vol. 52, No. 3, 502–511, May 2003.
16. Min, S. and H. L. Bertoni, "Effect of path loss on CDMA system design for highway microcells," *Proc. 48th IEEE Vehicular Technology Conference*, 1009–1013, Ottawa, Canada, May 1998.
17. Anang, K. A., P. B. Rpajic, T. I. Eneh, and B. Lawal, "Sensitivity of information capacity of land mobile cellular system to propagation loss parameters at higher microwave frequencies," *Proc. 7th IEEE International Wireless Communications and Mobile Computing Conference*, 630–635, Istanbul, Turkey, Jul. 2011.
18. Sánchez, M. G., I. Cuinas, and A. V. Alejos, "Electromagnetic field level temporal variation in urban areas," *IET Electronics Letters*, Vol. 41, No. 5, 233–234, Mar. 2005.
19. Nešković, A., N. Nešković, and D. Paunović, "Macrocell electric field strength prediction model based upon artificial neural networks," *IEEE J. Select. Areas Commun.*, Vol. 20, No. 6, 1170–1176, Aug. 2002.

20. Harley, P., "Short distance attenuation measurements at 900 MHz and 1.8 GHz using low antenna heights for microcells," *IEEE J. Select. Areas Commun.*, Vol. 7, No. 1, 5–11, Jan. 1989.
21. Rustako, A. J., N. Amitay, G. J. Owen, and R. R. Roman, "Radio propagation at microwave frequencies for line-of-sight microcellular mobile and personal communications," *IEEE Trans. Veh. Technol.*, Vol. 40, No. 1, 203–210, Feb. 1991.
22. Domazetovi, A., L. J. Greenstein, N. B. Mandayam, and I. Seskar, "Propagation models for short-range wireless channels with predictable path geometries," *IEEE Trans. Commun.*, Vol. 35, No. 7, 1123–1126, Jul. 2005.
23. ITU, "Propagation data and prediction methods for planning of short-range outdoor radiocommunication systems and radio local area networks in the frequency range 300 MHz to 100 GHz," Recommendation ITU-R P.1411-1, ITU Radiocommunication Assembly.
24. Clark, M. V., V. Erceg, and L. J. Greenstein, "Reuse efficiency in urban microcellular networks," *IEEE Trans. Veh. Technol.*, Vol. 1, 421–425, Apr. 1996.
25. Cuinas, I. and M. G. S'anchez, "Wide-band measurements of nondeterministic effects on the bran indoor radio channel," *IEEE Trans. Veh. Technol.*, Vol. 53, No. 4, 1167–1175, Jul. 2004.
26. Alouini, M. and A. J. Goldsmith, "Area spectral efficiency of cellular mobile radio systems," *IEEE Trans. Veh. Technol.*, Vol. 48, No. 4, 1047–1065, Jul. 1999.
27. Lee, W. C. Y., *Mobile Communication Design Fundamentals*, 142, John Wiley & Sons, New York, 1993.
28. Lee, W. C. Y., "Elements of cellular mobile radio systems," *IEEE Trans. Veh. Technol.*, Vol. 35, No. 2, 48–56, May 1986.
29. Anang, K. A., P. B. Rpajic, T. I. Eneh, and Y. Nijasure, "Minimum cell size for information capacity increase in cellular wireless network," *Proc. 73rd IEEE Vehicular Technology Conference*, 305–311, Budapest, Hungary, May 2011.